

Quantum Sensing with Squeezed Light

B. J. Lawrie,^{*,†} P. D. Lett,^{*,‡} A. M. Marino,^{*,¶} and R. C. Pooser^{*,§}

[†]Quantum Information Science Group, Computational Science and Engineering Division, Oak Ridge National Laboratory, Oak Ridge, Tennessee 37831, United States

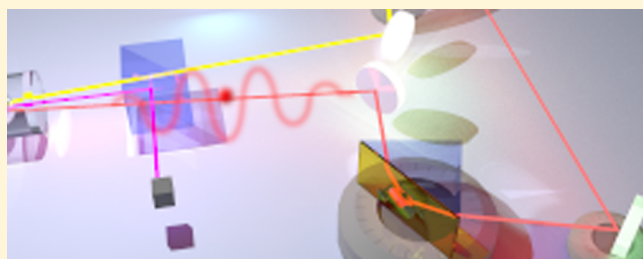
[‡]Joint Quantum Institute, National Institute of Standards and Technology and the University of Maryland, College Park, Maryland 20742, United States

[¶]Homer L. Dodge Department of Physics and Astronomy, The University of Oklahoma, Norman, Oklahoma 73019, United States

[§]Quantum Information Science Group, Computational Science and Engineering Division, Oak Ridge National Laboratory, Oak Ridge, Tennessee 37831, United States

ABSTRACT: The minimum resolvable signal in sensing and metrology platforms that rely on optical readout fields is increasingly constrained by the standard quantum limit, which is determined by the sum of photon shot noise and back-action noise. A combination of back-action and shot noise reduction techniques will be critical to the development of the next generation of sensors for applications ranging from high-energy physics to biochemistry and for novel microscopy platforms capable of resolving material properties that were previously obscured by quantum noise. This Perspective reviews the dramatic advances made in the use of squeezed light for sub-shot-noise quantum sensing in recent years and highlights emerging applications that enable new science based on signals that would otherwise be obscured by noise at the standard quantum limit.

KEYWORDS: quantum sensing, squeezing, quantum noise reduction, continuous variable quantum optics



Quantum optics is undergoing a renaissance in terms of its applicability to sensing platforms in a growing number of fields. Quantum noise reduction or “squeezing” occurs when the statistical noise in one variable of a quantum field is reduced at the expense of increased noise in the conjugate variable (Figure 1). This effect can be used to increase the signal-to-noise when detecting physical phenom-

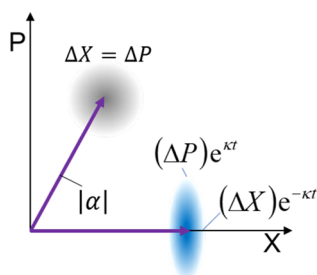


Figure 1. For a coherent state, the gray “fuzz ball” in the schematic represents symmetric uncertainty in the quadratures X and P at the standard quantum limit. For a squeezed state, the blue uncertainty ellipse is smaller along one quadrature axis and larger along the other. For the case shown, the squeezed and antisqueezed quadratures are X and P , respectively, but in general, any linear combination can be squeezed. The parameter κ , which determines the strength of the squeezing, is a property of the nonlinear system that facilitates interaction between optical fields.

ena that transduce the squeezed variable. More than 30 years after the first observations of quantum noise reduction from squeezed light sources^{1–5} and the first proof-of-principle squeezed quantum sensors,^{6–8} increasingly practical quantum sensors can now beat classical sensors whose state-of-the-art sensitivity is constrained by the Heisenberg uncertainty principle.^{9–11} In the intervening years, sensors based on quantum optics have typically demonstrated useful proofs of principle, but the observable quantum effects have, until very recently, been so small that the minimum resolvable signal was no better than the optimal classical configuration.

Over the past decade, squeezing has become increasingly essential to the characterization of plasmonic sensors^{12–14} that are susceptible to photothermal modulation and damage above milliwatt optical powers and to the characterization of micromechanical sensors^{9,15} where back-action noise exceeds photon shot noise for similar optical powers. The inclusion of squeezed light into magnetometers could also improve on the state of the art, though squeezed atomic magnetometers have thus far not exceeded the sensitivity of conventional atomic magnetometers. In all of these cases, back-action noise and thermal feedback provide a hard limit on increased optical

Received: February 12, 2019

Revised: May 11, 2019

Accepted: May 13, 2019

Published: May 13, 2019

power, and quantum noise reduction in squeezed optical states provides a path toward improved sensitivity that cannot be achieved through classical means. Other techniques have been developed that take advantage of correlations present in squeezing and entanglement even in the presence of large losses, but these quantum illumination schemes are beyond the scope of this Perspective.^{16–19}

The above sensing examples are limited to single-channel or two-channel measurements. With a single sensor, the devices can only lend the benefit of quantum correlations to a single position, while a physical field of interest may be spread over a wide area, across a classical network of sensors. The next generation of quantum sensors will take advantage of quantum networks in which the quantum sensors are linked to one another through quantum mechanical means, typically via entanglement.²⁰ Ultimately, quantum networks should be capable of $1/N$ scaling in uncertainty, where N is the number of quantum resources, such as photons, modes, or detectors.²¹ This limit can be reached with perfect entanglement between sensing fields with N excitations, to be contrasted with the classical noise scaling at the shot noise level (SNL), $1/\sqrt{N}$. Here, we present a review of practical quantum sensors that leverage quantum noise reduction to enable fundamentally new approaches to sensing and metrology in fields as diverse as high energy physics, biochemistry, and scanning probe microscopy.

■ QUANTUM NOISE REDUCTION IN SQUEEZED LIGHT SOURCES

The first proposal for quantum sensors based on quantum optics leveraged quantum noise reduction or “squeezing”.⁵ Squeezed light sources rely on the asymmetric distribution of uncertainty between conjugate variables of the optical field, such as the amplitude, X , and phase, P , quadratures (see Figure 1) of minimum uncertainty states that saturate the Heisenberg uncertainty principle with $\Delta X \Delta P = 1$. The coherent state is a special case of minimum uncertainty states in which the uncertainty is evenly distributed between the two quadratures. In contrast, the uncertainty of one quadrature of a squeezed state can be arbitrarily small at the expense of increased uncertainty of the other quadrature, as shown in Figure 1. In general, a medium is required to facilitate the nonlinear optical interactions which lead to squeezing. These media are characterized by a nonlinear parameter κ , which determines the strength of the squeezing after some interaction time within the medium.

This classically inaccessible control over the uncertainty of quadratures of the optical field has clear implications for sensing. Any sensor that is normally characterized by modulations imparted on the amplitude or phase quadratures (or linear combinations thereof) of an optical readout field can in principle be augmented by squeezing the amplitude or phase quadrature (or the appropriate linear combination). Not only does squeezing offer higher signal-to-noise ratios (SNRs), it may enable one to detect signals that were not visible at all in the analogous classical sensor.

The aforementioned nonlinear media can be engineered to cause disparate fields to interact—the nondegenerate or two-mode case—or to cause a field to interact with itself—the degenerate or single-mode case. Single-mode squeezed states have been used extensively for quantum sensing.^{15,22–29} Multimode squeezing opens up entirely new fields of study

in quantum information science beyond conventional quantum sensing,^{9,10,14,30–34} including quantum networking and communications,^{35–37} entanglement,^{38–40} and quantum computing,^{41–47} none of which is possible with single-mode squeezed states alone (although single-mode squeezing may be used as a resource for the generation of multimode squeezed states).

■ FUNDAMENTALS OF QUANTUM SENSING WITH SQUEEZED LIGHT

The problem of sensing is directly related to parameter estimation. In general, a system sensitive to the quantity being measured is used as the sensor, and this sensor is then probed to extract the information on the measurement. For optically transduced sensors, light is used to probe the system performing the measurement and the information is extracted through measurements of a given property of the light, such as its amplitude or phase quadrature.

The sensitivity of the whole sensing apparatus is then characterized as the inverse of the minimum resolvable signal, ΔP_{\min} , that can be detected for the parameter P being estimated. This minimum resolvable signal can be related to the property of the light that is being measured and the properties of the measurement system through the following relation:

$$\Delta P_{\min} = \frac{1}{\sqrt{N}} \frac{1}{|\partial M / \partial P|} \frac{\sqrt{\langle (\Delta L)^2 \rangle}}{|\partial L / \partial M|} \quad (1)$$

where M is the property of the measurement system that changes given a change in the parameter being measured, L is the property of the light that is measured to extract the information, and N is the number of times the measurement is performed.¹⁰ In this expression, the term $|\partial M / \partial P|$ characterizes how much the measurement system changes with a change of parameter P and the term $\langle (\Delta L)^2 \rangle$ corresponds to the noise of the light used to probe the measurement system.

If we consider the case of intensity, I , measurements, the role of quantum noise reduction can be seen if we rewrite eq 1 in terms of the squeezing level $S = \langle (\Delta I)^2 \rangle / \langle I \rangle$, such that

$$\Delta P_{\min} = \frac{1}{\sqrt{N}} \frac{1}{\beta |\partial M / \partial P|} \sqrt{\frac{S}{\langle I \rangle}} \quad (2)$$

where we have assumed that the interaction between the light and the measurement system is linear, such that $|\partial I / \partial M| = \beta \langle I \rangle$, where β is a proportionality constant. An analogous statement can be written for measurements based on other properties of the light. Given that S decreases as the level of squeezing increases, we can see that a larger level of squeezing will result in a smaller minimum resolvable signal. As a result, the sensitivity (inverse of the minimum resolvable signal) increases with the level of squeezing and with the number of photons in the light used to probe the measurement system. Thus, for a given measurement system, the use of squeezed light as a resource becomes relevant when it is not possible to increase the amount of light that can be used to probe it. At this point, quantum states of light offer the only viable option for further sensitivity enhancements.

It is important to note that eq 2 describes measurements that use only a single quadrature of the optical field. Further improvements in sensitivity can be achieved if an optimal measurement strategy can be identified. In this case, it is in

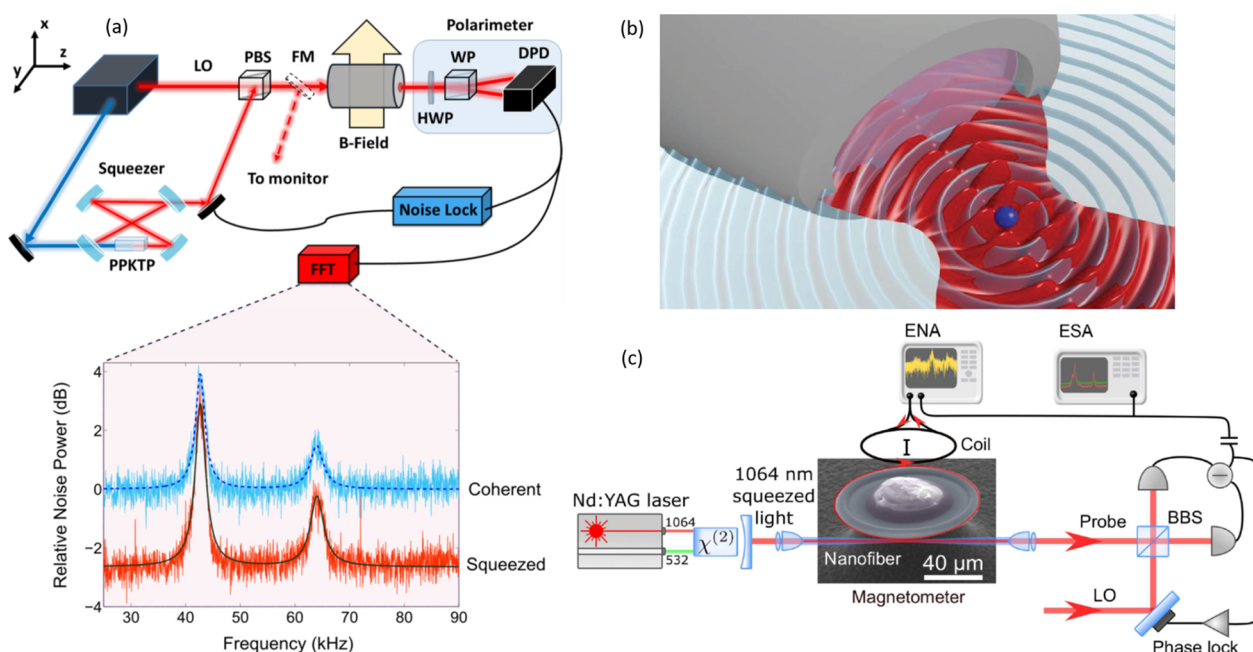


Figure 2. Quantum-enhanced sensing with single-mode squeezing. (a) The use of polarization squeezing has been shown to enhance magnetometers based on Faraday-rotation in an atomic system.⁵¹ (b) Squeezed light can lead to enhanced biological measurements, where the power that can be used to probe the sample is limited due to the possibility of damage.²² Here, naturally occurring lipid granules are tracked in real time by interfering scattered light with a squeezed local oscillator enabling sensitivity beyond the SNL, or quantum noise limit. The graphic illustrates the scattered light from a trapped particle (light blue) interfering with a local oscillator (red) and collected by a microscope objective. (c) The interface between squeezed light and micromechanical systems offers the possibility of measuring different physical quantities beyond the SNL, including local magnetic fields when magnetostrictive materials are deposited on micromechanical resonators.⁵²

principle possible to reach the ultimate limit in sensitivity given by the quantum Cramér–Rao bound.⁴⁸

■ QUANTUM SENSING WITH SINGLE-MODE SQUEEZING

To produce squeezed light, a nonlinear optical medium is required. Such media result in nonlinear interaction Hamiltonians in the Heisenberg picture of the form $H = i\chi^{(2)}a_i a_j a_p^\dagger + \text{H.C.}$ for a second-order nonlinear medium, where $\chi^{(2)}$ is a material property related to the nonlinear polarizability, a_{ij} are the quantum annihilation operators for two optical fields that interact with a third field a_p , which is referred to as the pump and provides energy for the interaction, and H.C. is the Hermitian conjugate of the preceding term. Throughout this Perspective, units are defined in terms of $\hbar = 1$. The pump field is generally much stronger than the other fields and is thus often taken to be classical, such that $\chi^{(2)}\alpha_p = \kappa$, where α_p is the electric field amplitude of the pump. When $i = j$, the interaction is degenerate, and one obtains a simpler interaction Hamiltonian, $H = i\kappa(a^2 - a^{\dagger 2})$, which leads to single-mode squeezed states. The precise noise reduction obtained by a given Hamiltonian can be found by solving the Heisenberg equation of motion for the quantized field: $\dot{a} = -i[a, H]$, which leads to $\dot{a} = -2\kappa a^\dagger$ and hyperbolic sinusoidal solutions. Defining the electric field quadratures as $X = a + a^\dagger$ and $P = i(a - a^\dagger)$, one has exponential solutions as a function of time for real κ

$$P(t) = e^{2\kappa t}P(0) \quad (3)$$

$$X(t) = e^{-2\kappa t}X(0) \quad (4)$$

which lead to the variances

$$\langle \Delta P(t)^2 \rangle = e^{2\kappa t} \langle \Delta P(0)^2 \rangle \quad (5)$$

$$\langle \Delta X(t)^2 \rangle = e^{-2\kappa t} \langle \Delta X(0)^2 \rangle \quad (6)$$

That is, for $t > 0$ the variance of the amplitude quadrature of the electric fields decreases exponentially from some starting value, while the phase quadrature variance increases commensurately. This is the mathematical definition of single-mode amplitude squeezing. These ideas can be extended to different degrees of freedom of the light, such as the polarization.

The initial proposal to use squeezed light for quantum sensing was based on the notion of taking advantage of the reduced noise property of single-mode squeezed states of light to enhance the sensitivity of an interferometer.^{5,49} This has been one of the most studied applications for quantum enhancement with squeezed light and has now found its way into gravitational wave observatories, such as LIGO and GEO 600,^{11,50} for further sensitivity enhancements. There have also been a number of sensing applications beyond interferometers that take advantage of single-mode squeezed light that have been proposed and implemented (see Figure 2 for a few examples). It is important to note that one of the main constraints with the use of squeezed light for sensing applications is the degradation of the level of squeezing and, thus, of the degree of enhancement that can be obtained with losses. This has frequently limited the use of squeezed light for sensing to proof-of-principle experiments.

The ability to use squeezed light to enhance sensing requires an optically transduced sensor that already operates at the SNL with a classical readout field. Given the control that can be achieved with atomic systems, their sensitivity to different physical quantities, and the ability to efficiently probe them

with light, many sensing configurations are based on atomic systems with optical readouts. This has led to a number of proposals and experiments that combine squeezed light and atomic systems for quantum-enhanced sensing. It has been proposed that squeezing can enhance the sensitivity of atomic interferometers,⁵³ which could lead to enhancements in the precision of atomic clocks and measurement of acceleration, rotation, and gravity gradients. The use of atomic systems has led to some of the most precise sensing devices for electromagnetic fields. For example, atomic magnetometers have achieved sensitivities below 1 fT/ $\sqrt{\text{Hz}}$.⁵⁴ Several experiments have shown that such devices can be further enhanced through the use of polarization squeezed light,^{55,56} which can be generated by mixing two quadrature squeezed beams on a polarizing beamsplitter.⁵⁷ More recently, it has been shown that squeezed light can also enhance the sensitivity of spin noise spectroscopy, which can be used to determine fundamental properties of spin systems in thermal equilibrium.⁵⁸ Experiments with an initial polarization squeezed state exhibiting 3.0 dB of squeezing have shown enhancements in the signal-to-noise ratio of up to 2.6 dB for Faraday-rotation-based spin noise spectroscopy, see Figure 2a.⁵¹

One of the applications in which the use of squeezed light can lead to practical enhancements is the probing of biological samples. In this case, the amount of power that can be used to probe the biological samples has to be limited in order to avoid damage. As a result, some biosensing devices are power constrained and the only way to further enhance their sensitivity is through the use of quantum resources. With this idea in mind, recent experiments have shown that squeezed states of light are compatible with biological measurement techniques, see Figure 2b.²² In particular, these experiments used squeezed light with reduced amplitude noise to perform microrheology experiments surpassing the SNL by 42%.

The interface between squeezed light and optomechanical systems also offers exciting possibilities for quantum enhanced sensing of acceleration, mass, and electromagnetic fields. For example, a recent theoretical proposal studied the use of an optomechanical system coupled to a cold atomic ensemble inside a cavity injected with vacuum squeezed light for the detection of forces below the standard quantum limit.⁵⁹ It has also been experimentally shown that it is possible to measure the optomechanical motion and forces associated with an object beyond the ultimate bound (Cramér–Rao bound) for a coherent state. In particular, by probing the motion of a mirror under external stochastic forces with phase squeezed light, enhancements of 15% and 12% for the position and momentum estimations of the mirror, respectively, and of 12% for the force were achieved.⁶⁰ More recently, through the use of a microcavity optomechanical device, see Figure 2c, a silicon-chip based magnetometer with a quantum enhancement in the magnetic field sensitivity of 20% and an effective increase in bandwidth of 50% was experimentally implemented.⁵²

The enhancements that can be obtained in the time domain through the use of single-mode squeezing can also be extended to the spatial domain for quantum states of light that exhibit spatial quantum correlations, or spatial squeezing. Among other things this makes it possible to estimate the pointing direction of a laser below the SNL.²⁴ This capability can lead to enhancements of devices that require measuring beam positioning, such as an atomic force microscope. Spatial

squeezing has also been used in proof-of-principle experiments to show improved spatial resolution for biological applications. Through the application of squeezed light in a photonic-force microscope a 14% enhancement in resolution was achieved with respect to the corresponding configuration using classical resources.²³

It has been shown in theory that, for Gaussian quantum states, the maximum level of enhancement can be obtained by placing all the squeezing in the correct single mode, either temporal or spatial.³⁴ However, the use of two-mode squeezed states or twin beams can offer an advantage in the presence of classical technical noise due to the ability to perform a differential measurement that can cancel the classical noise.

■ QUANTUM SENSING WITH TWO-MODE SQUEEZING

While many groups have explored quantum sensing with single-mode squeezed states of light, quantum sensors based on two-mode squeezing in which either the amplitude-difference or the phase-sum quadratures are squeezed have recently been shown to provide a significantly more accessible approach to quantum sensing. The majority of these quantum sensing demonstrations have relied on the use of intensity-difference squeezing generated by four-wave mixing. A description of the quantum noise reduction present in this class of quantum sensors can be calculated analytically in terms of the Heisenberg picture description of the input and output operators for the four-wave mixing process.^{9,10,31,33,61} In this case, the interaction Hamiltonian is given by $H = i\chi^{(3)}a_1a_2a_p^\dagger a_p^\dagger + \text{H.C.}$ In the experiments described in this Perspective, the pump field is powerful relative to the other fields and is undepleted for the experimental parameters used here, which result in nonlinear gains from 2 to 20. Thus, the process is very similar to a second-order nonlinear optical process in which the pump is undepleted, with $\kappa = -\chi^{(3)}\alpha_p^2$. Considering sums and differences of the quadratures, one has the Heisenberg equations of motion

$$\dot{P}_1 + \dot{P}_2 = -\kappa(P_1 + P_2) \equiv \dot{P}_+ \quad (7)$$

$$\dot{X}_1 - \dot{X}_2 = -\kappa(X_1 - X_2) \equiv \dot{X}_- \quad (8)$$

For real κ , these equations lead to solutions that are exponential in time

$$P_+(t) = e^{-\kappa t} P_+(0) \quad (9)$$

$$X_-(t) = e^{-\kappa t} X_-(0) \quad (10)$$

whose variances are each squeezed, analogous to the single-mode case. Thus, the two-mode squeezed case is a simple generalization of the single-mode case presented previously, with the squeezing now shared between separate optical modes. These shared correlations are a signature of entanglement, which is useful for quantum networking.

Plasmonic sensors may be the most ubiquitous class of proof-of-principle quantum sensors to utilize two-mode squeezed light. Classically, plasmonic sensors rely on the sensitivity of plasmons, quasiparticles resulting from the resonant oscillations of free electrons, to changes in the local refractive index. Small changes in refractive index due to ligands bound to analytes on a metal surface modify the plasmon resonance. Spectrally, polarization, or angular resolved measurements of the shift in plasmon resonance enable detection of small concentrations of molecules.

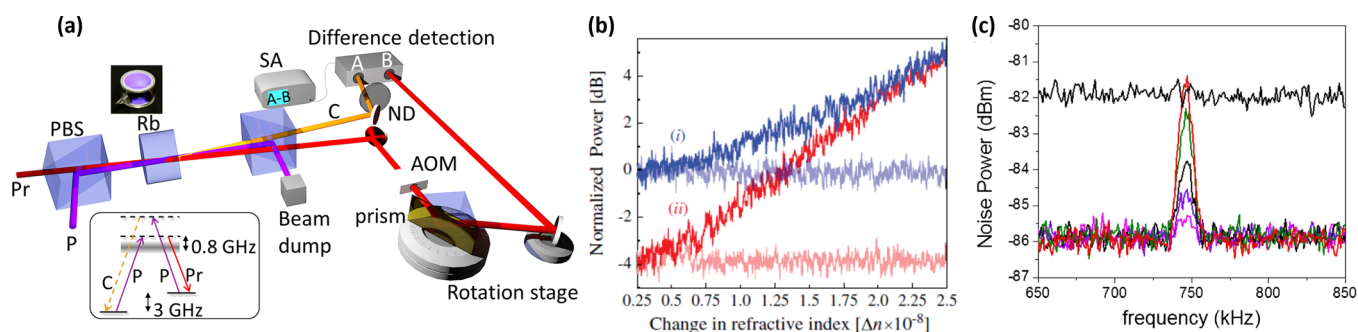


Figure 3. (a) Schematic of quantum sensing with four-wave mixing of noncollinear pump (P) and probe (Pr) fields in ^{85}Rb . The measured intensity difference between the probe and conjugate (C) shows quantum noise reduction on a spectrum analyzer (SA).³³ Modulating the probe field amplitude with an acousto-optic modulator before transducing the response of a plasmonic Kretschmann sensor enables the subsequent demodulation of the plasmonic sensor response on the spectrum analyzer with a noise floor below the SNL. (b) A variation of this quantum plasmonic sensor illustrated a 4 dB enhancement in the sensitivity to changes in refractive index in plasmonic sensors operating with squeezed light readout (ii) compared with coherent readout (i).¹⁰ (c) Microcantilever beam displacement measurements performed with multispatial mode squeezed light resulted in the demonstration of $\text{fm}/\sqrt{\text{Hz}}$ displacement sensitivity 4 dB below the SNL (variable displacement amplitudes are illustrated in different colors).⁹ This approach enables classically inaccessible measurements of microcantilever beam-displacement for measurements detuned from the micromechanical resonance frequency, but thermal noise continues to limit measurements on-resonance.

Quantum plasmonics has experienced increased growth as a field in recent years due to advances in nanoimaging,⁶² subwavelength photonic circuits,⁶³ and general interfacing of quantum systems with plasmons.^{13,64} Conventional plasmonic sensors have been shown to operate at the SNL, with a demonstration of 4×10^{-9} refractive index unit (RIU) sensitivity based on extraordinary optical transmission (EOT) of classical light sources through subwavelength hole arrays.⁶⁵ High optical powers can detrimentally affect a variety of plasmonic sensors. For example, photosensitive ligands and plasmonic saturation effects frequently constrain the maximum laser transduction power.⁶⁶ In these cases, squeezed light is ideal for increasing the SNR without increasing the optical power.

It is worth noting here that amplitude squeezing of a coherent state without amplification would result in reduced optical power because of the reduced variance illustrated in Figure 1. However, because most practical squeezed states rely on nonlinear amplifiers, the output power of the squeezed state is typically substantially larger than that of the coherent seed field. Thus, any comparison of the power of squeezed light sources and coherent light sources must consider the power in the squeezed state after the nonlinear amplifier.

Several groups have now demonstrated that localized and propagating surface plasmon modes can coherently transduce single-mode and multimode squeezed states of light with loss of squeezing simply modeled by a beamsplitter interaction equivalent to the plasmonic loss.^{13,37,67} In the wake of those results, the idea of using squeezed states of light to enhance the sensitivity of plasmonic sensors has gained significant traction.^{10,14,31,33} State-of-the-art classical plasmonic sensors utilize differential detection with a reference field that does not interact with the plasmon in order to eliminate noise present in the probe laser.⁶⁸ Many of these sensors are now limited by the SNL, and quantum sensors will be required for further improvements in sensitivity.

Figure 3a illustrates a typical two-mode quantum sensing design.³³ In this example, the probe beam generated by a four-wave mixing process replaced the standard laser readout within a plasmonic sensor (operating in a Kretschmann configuration⁶⁹). In classical, shot-noise limited, balanced photodetection, subtracting a reference channel from the probe

removes classical noise sources but causes the shot noise of the two channels to add in quadrature. In contrast, the balanced photodetection illustrated in Figure 3a subtracts both classical noise and the shared quantum correlations between the probe and conjugate fields, resulting in quantum noise reduction below the SNL. As with classical balanced photodetection, modulation and demodulation of the probe enables the signal to be monitored on the sideband frequency. In this example, an acousto-optic modulator was used to impart a sideband signal at 1.5 MHz, and a spectrum analyzer was used to monitor that sideband as the refractive index near the gold film was varied. A variable neutral density filter introduced loss on the conjugate field equal to the loss on the probe field in order to maximize the quantum noise reduction in the system. A similar approach was used to demonstrate state-of-the-art sensitivity of 6.8×10^{-10} RIU/ $\sqrt{\text{Hz}}$ in an EOT-based sensor,¹⁰ as shown in Figure 3b.

For each of these quantum plasmonic sensors, a large amount of squeezing is observed near the inflection points of the angle or spectrally resolved transmission spectrum, meaning that one can choose to operate the sensor with a fixed wavelength and incidence angle⁶⁸ rather than operating at a point of maximum loss. At all points on the plasmonic response function, a higher SNR was achieved than is possible with the classical version of each sensor. The quantum light source used here can be operated at powers equal to those used in equivalent classical sensors because the classical sensor cannot be used at powers beyond the point of thermal modulation⁷⁰ of the plasmon or the damage threshold of photosensitive ligands.⁷¹ These thresholds are easily within the limits of typical squeezed light sources.

The recent demonstration of microcantilever beam displacement measurements below the SNL also relied on two-mode squeezing generated by four-wave mixing.⁹ Figure 3c illustrates the measurement of the displacement of a microcantilever for varying piezo-electric driving amplitudes with a two-mode squeezed light readout field, resulting in a minimum resolvable displacement of $1.56 \text{ fm}/\sqrt{\text{Hz}}$. As discussed above, seminal work in this area combined two single-mode squeezed states and an intense coherent field in orthogonal transverse modes to characterize the displacement of a mirror with sensitivity

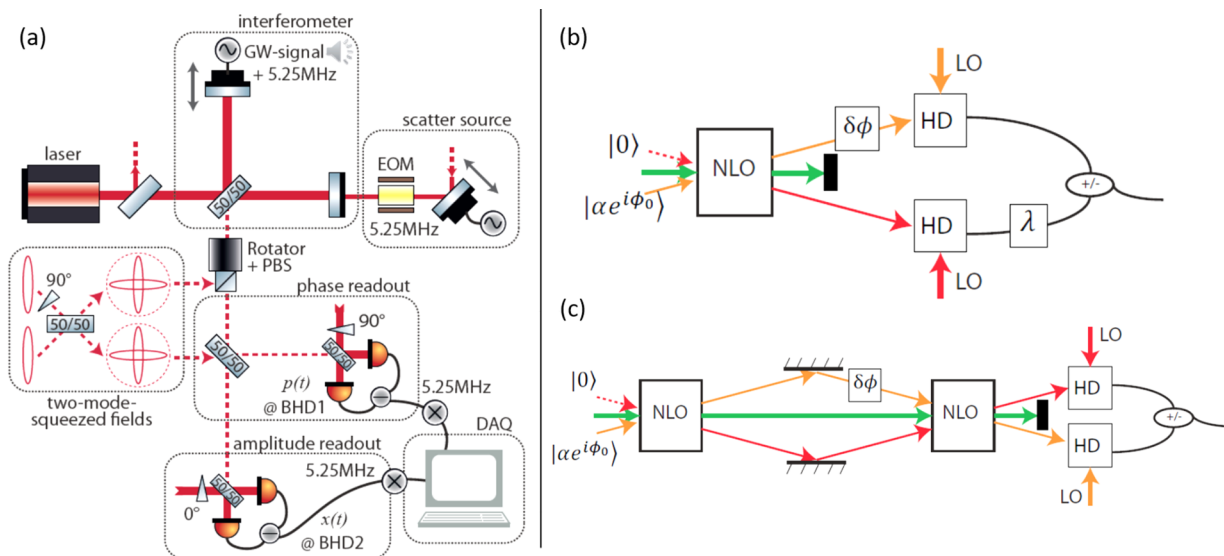


Figure 4. (a) An interferometer with two-mode squeezed states applied to the readout, which is a simple extension of the typical single-mode squeezed light readout.⁸² Here, a simulated gravitational wave (GW) signal was generated with a piezo-modulated interferometer mirror, two-mode squeezed states were injected into the Michelson interferometer, and dual balanced homodyne detectors (BHD1 and BHD2) were used to read out the amplitude and phase quadratures. (b) A truncated SU(1,1) interferometer and (c) the more common nonlinear interferometer in the Mach–Zehnder configuration.⁸³ In panels b and c, the beamsplitters that were used in panel a are replaced with a four-wave mixing process in nonlinear optical (NLO) media but a similar dual homodyne detection (HD) approach is used to read out the amplitude and phase quadratures.

below the SNL.²⁴ The two-mode squeezing beam displacement measurement simplified this approach because the four-wave mixing process generated squeezing in several coherence areas within the probe and conjugate beams, removing the need to coherently combine multiple transverse modes.⁹ This spatial distribution of quantum correlations may enable new quantum-enhanced atomic force microscopies. Interestingly, it can also be described as a truncated nonlinear interferometer because of the equivalence between the split photodetection used for these beam displacement measurements and dual homodyne detection.⁷²

The spatial distribution of quantum correlations in the four-wave mixing process is also critical to the development of quantum-enhanced imaging, as it leads to relative spatial squeezing between the probe and the conjugate.⁷³ Recent explorations of the distribution of coherence areas within the probe and conjugate beams have shown that the level of squeezing can vary dramatically across the two beams.⁷⁴ Control over that spatial distribution of correlations⁷⁵ has enabled quantum imaging that takes advantage of the quantum correlations between the probe and conjugate channels to reveal images that are difficult to detect with both photodiodes and single-photon detectors.^{76,77} This approach to quantum imaging with two-mode quantum states has also been realized with a spontaneous parametric downconversion source.³⁰ Another variant on quantum imaging has amplified images in the four-wave mixing process as part of the development of networks of bipartite squeezed or entangled states that are encoded within the amplified image.^{12,37,38}

Two-mode squeezed states are frequently understood to suffer from a 3 dB “penalty” compared with single-mode squeezed states because roughly half of the power of the squeezed state is in the conjugate field. However, there are an increasing number of demonstrations in which that penalty may be irrelevant or taken advantage of. For instance, a recent demonstration of quantum plasmonic sensing transduced the plasmonic sensor response with quantum noise itself rather

than the RF sideband of the probe field.¹⁴ There, the probe field interacted with the plasmonic sensor before photodetection while the conjugate field was detected directly by a balanced photodetector. When off-resonance, the probe was not absorbed by the plasmon, and the measured noise was 5 dB below the SNL. When on-resonance, the probe was strongly absorbed, and the quantum anticorrelations resulting from that asymmetric loss resulted in a 5 dB increase in sensitivity compared with classical readout.

Another recent quantum sensor to take advantage of both modes in a two-mode squeezed state was an atomic magnetometer with in situ two-mode squeezing.⁶¹ In this demonstration, the strong coherence required for the four-wave mixing process also enabled nonlinear magneto-optical rotation on the probe and conjugate fields. Each mode exhibited the same RF polarization rotation response, but a slight misalignment of the probe and conjugate beams on a pair of polarizers resulted in the translation of the identical polarization modulations into out-of-phase amplitude modulations. Thus, balanced photodetection resulted in the subtraction of the quantum correlated noise below the SNL, while the signals on each beam added. That is, the intensity difference noise was 4.7 dB below the SNL, while the differenced signal was equal to the sum of the signal on the probe and conjugate.⁶¹ Interestingly, these approaches to multimode quantum sensing also offer the potential for vector field sensing that would be impossible to achieve with single-mode squeezing.

■ INTERFEROMETRY WITH SQUEEZED LIGHT SOURCES

Single-mode squeezed light implies reduced noise or fluctuations in either the phase or amplitude quadrature of a beam of light. For a given optical intensity, this feature can be used to increase the sensitivity of interferometers, as highlighted in Figure 4a for two-mode squeezed states.

There are a number of different ways to achieve this goal. A typical Mach–Zehnder interferometer has light injected into two orthogonal arms through one port of a beamsplitter; the other “open” port of the beamsplitter can be viewed as allowing a vacuum field into the interferometer and with it the associated vacuum noise. This noise is typically small, but in today’s world of increasing sensitivity, it can become the limiting noise in a measurement. The vacuum noise can be reduced by deliberately injecting squeezed light instead of allowing the vacuum to enter.

Under normal circumstances, it is easier to increase the sensitivity of an interferometer measurement by using more laser power. The sensitivity of a classical interferometer that is limited by shot noise will have a sensitivity that scales with the inverse of the square-root of the power used in the interferometer, as shown in eq 2 for $S = 1$. Thus, turning up the power is often a cost-effective way to improve the sensitivity of an interferometer. Unfortunately, this is not always possible. Either because turning up the power will cause damage—for instance to biological samples—or because the system is already at the maximum power possible because of materials and other design considerations. Ideally, with squeezed light (and without losses and other complications), the sensitivity can instead scale as the inverse of the circulating power,⁴⁸ though decoherence and optical losses generally constrain the improvement.⁷⁸ This is the situation for gravitational-wave observatories, such as LIGO, the most notable application of squeezed light to date. In this case, a large investment has created a highly sensitive interferometer that is operating at the maximum internal power possible, and the injection of squeezed light into the interferometer can potentially increase the sensitivity without redesigning the device.^{11,50}

Interferometers, such as LIGO, are limited by shot noise at higher frequencies, and by radiation pressure fluctuations at low frequencies. Thus, phase squeezing is required at high frequencies, and amplitude or intensity squeezing is required at low frequencies to improve the sensitivity of measurements at all frequencies. Methods of rotating squeezing from one quadrature to another can be used to accomplish this (for instance by reflecting the light off of a detuned cavity).^{79–81} For most measurement applications, however, noise can be measured at a single frequency and choosing the appropriate quadrature to lock to will reduce the minimum resolvable phase in the interferometer.

Another class of quantum interferometers are those of the SU(1,1) variety, where instead of injecting squeezed light into the device, squeezing is generated by nonlinear elements within the interferometer itself, as seen in Figure 4b and c. In particular, two-mode squeezed light can be used to generate “twin beams” of light in the two arms of an interferometer. Such quantum states can also lead to increased sensitivity in phase measurements.⁸⁴ Two-mode squeezing creates phase and amplitude correlations between two beams of light. While the individual beams of light may be more noisy than a coherent state, one can essentially make a phase measurement with a noisy beam, and then remove much of the noise from the measurement by referencing it to its almost-identically noisy twin beam.

The original SU(1,1) interferometer proposal envisioned a Mach–Zehnder interferometer with the beamsplitters replaced by parametric amplifiers.⁸⁴ The first (phase insensitive) amplifier creates correlated pairs of photons in the

interferometer arms, which are then directed into a second, phase-sensitive amplifier. A phase shift on the pump beam makes this amplifier convert the correlated pair of photons back into pump photons. Thus, there is no output signal unless there is an additional phase shift in the interferometer. A seeded version of this interferometer was constructed using four-wave mixing in Rb vapor and used to demonstrate the fundamental signal gain and reduced noise that can be obtained in such a system.⁸⁵ Also using four-wave mixing in Rb vapor, a truncated version of the SU(1,1) interferometer that combined a phase-insensitive amplifier generating twin beams of light with homodyne detectors was demonstrated with a phase sensitivity improvement of 4 dB over the equivalent Mach–Zehnder interferometer.⁸⁶ Since losses in the interferometer severely limit the advantage that can be attained in practice, this scheme has the advantage of eliminating the second amplifier/vapor cell. Additionally, an SU(1,1) interferometer employing parametric downconversion with collinear pump and downconverted beams utilized direct detection with straightforward pump filtering in order to realize a more compact platform. This device demonstrated an improvement in phase sensitivity over the classical case of 2.3 dB.⁸⁷ Finally, fiber-optic nonlinear interferometers have recently been developed as part of the effort to make quantum sensors more useful for sensing in the field.^{88,89} As with the quantum sensors discussed above, these nonclassical interferometers have their advantage over their classical counterparts for the same number of phase-sensing photons.

■ DISTRIBUTED SENSING ACROSS QUANTUM NETWORKS

The experiment presented by Holtfrerich et al.³⁷ is unique in that it transmits quantum correlations through distant plasmons on independent substrates—it is an example of a small quantum network. Quantum optical networks are collections of physically separated optical modes related by a generalization of two-mode squeezing. In particular, quantum networks take advantage of the entanglement that two-mode squeezed states naturally exhibit. For globally distributed signals, which affect multiple nodes that are entangled, networked quantum sensors present an advantage over averaging independent sensors.⁹⁰ For this reason, networks of quantum sensors have been proposed as a natural way to obtain the Heisenberg limit in sensing, where noise scales inversely with the number of nodes on the network.⁹¹ Several types of quantum networks are possible, depending on the nature of the entanglement. Here, we describe two general networks. The first network type is called a Hamiltonian graph.⁹² The simplest implementation consists of a two-mode squeezed state, as described in the previous sections, with maximum squeezing. This configuration, also known as an Einstein–Podolsky–Rosen (EPR) state,⁹³ is a maximally entangled state. Hamiltonian graphs that are fully interconnected with equal weights describe Greenberger–Horne–Zeilinger (GHZ) states. In this case, the interaction between two fields, forming the edge of the graph, is given by $e^{-i\kappa_{ij}(a_i^\dagger a_j^\dagger - a_i a_j)}$, where κ_{ij} is the nonlinear coupling coefficient between fields i and j .

The equations of motion for the network in the Heisenberg picture can be written in matrix form

$$\dot{\mathbf{A}} = \boldsymbol{\kappa} \cdot \mathbf{A}^\dagger \quad (11)$$

where $\kappa = \kappa \begin{pmatrix} 0 & 1 \\ 1 & 0 \end{pmatrix}$ for example, for two modes. Here κ is an adjacency matrix. This network can easily be generalized to more than two modes by considering concurrent interactions between n modes in the network

$$H = i \sum_{i=1}^n \sum_{j \neq i}^n \kappa_{ij} (a_i^\dagger a_j^\dagger - a_i a_j) \quad (12)$$

The above Hamiltonian implies that all optical fields interact with specific strengths with all other fields in the network. For instance, six fields have a graph as shown in Figure 5. Any connectivity can be represented by tuning the adjacency matrix, which amounts to specifying a new Hamiltonian.

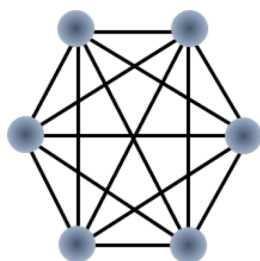


Figure 5. Six node fully interconnected Hamiltonian graph representing a GHZ state. The nodes are optical modes while the edges represent the entangling interaction.

Another useful network type is called a cluster graph. In this network, the edges represent different interactions, known as quantum nondemolition operators.^{94,95} The edges in a cluster graph are defined by $e^{iX_i P_j}$, where X and P are the amplitude and phase quadratures of each node on the graph.

The nodes in the cluster graph represent each field after a degenerate nonlinear interaction, which reduces the phase. That is, $P_i \rightarrow 0$. However, it is possible to represent the nodes on a cluster graph as equivalent to those in the Hamiltonian graph with a redefinition of the phase of a single field. One example of a cluster graph with long-range order is shown in Figure 6.

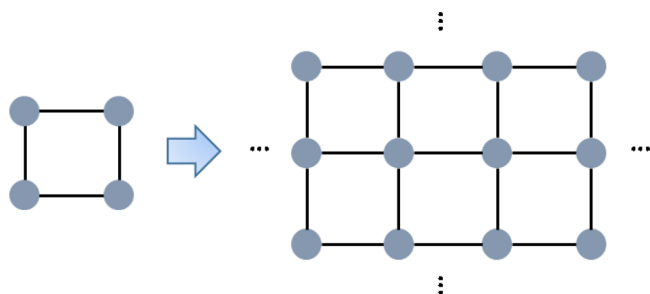


Figure 6. Square cluster state graphs. The single tile (left) can be repeated to achieve long-range order (right).

For cluster states, a node's phase depends on its neighbors' amplitudes, while neighboring amplitudes are independent. The equations of motion yield solutions $X_i(t) - P_j(t) = e^{-\kappa t} P_j(0)$ and $P_i(t) - X_j(t) = e^{-\kappa t} P_i(0)$. Application of a Fourier transform to one node of a cluster graph transforms it to a Hamiltonian graph. Under $X \rightarrow P$ and $P \rightarrow -X$, we have

$$X_1(t) + X_2(t) = e^{-\kappa t} P_2(0) \quad (13)$$

$$P_1(t) - P_2(t) = e^{-\kappa t} P_1(0) \quad (14)$$

As $t \rightarrow \infty$, eqs 13 and 14 and eqs 9 and 10 are identical up to an arbitrary, semantic, and local definition of quadrature, which has no effect on graph topology. This property is important because it allows one to construct experimentally the network which is easier to produce, and then adjust the measurements accordingly to produce either a GHZ state or a cluster state, depending on the quantum sensing application.

Multimode squeezing can be used to produce a network like that shown in Figure 6. Extending squeezing measurements to more than two modes is straightforward. For example, the GHZ state, which is a maximally entangled state, shows quantum noise reduction for specific quantum operators found by diagonalizing the adjacency matrix κ . For a k -mode GHZ state, the squeezed operators are

$$(k-1)X_1 - \sum_{i=2}^k X_i \quad (15)$$

$$\sum_{i=1}^k P_i \quad (16)$$

Thus, an advantage to SNR for a distributed signal across multiple nodes in the case of a phase signal requires a joint phase measurement and computing the joint phase sum quadrature. In the case of multimode squeezed spin networks, this measurement scheme is optimal.^{91,96,97} In the same way that two-mode squeezed states use a reference, which shares correlations with the signal beam, quantum networks can maintain large portions of the network as references (half of the nodes, for example, while half or more transduce a global signal). With these ideas in mind, we see that quantum networked sensing is a straightforward extension of sensing with two-mode squeezed states, and indeed the latter is a simple form of a quantum network. This realization provides a plausible path forward to the next generation of quantum sensing: multimode quantum noise reduction distributed across a network topology. We note that any plausible network should consider propagation losses in addition to the already commonly discussed detection efficiencies and other losses present in quantum sensing experiments. In quantum networks that use continuous-variable entanglement, lab-scale experiments will require some extra consideration, but propagation losses will be similar to typical sensing experiments. However, for large geographic networks focusing on entanglement distribution, quantum repeaters will ultimately be required to maintain high quantum correlations.

An additional complication arises in networks with large geographic separation: to perform quadrature measurements, a local oscillator is required (this requirement is not present if only intensity-type correlations are required for the sensing protocol, but this is a special case). In this regard, quantum networks with distributed entanglement bear a lot of similarities with continuous-variable quantum key distribution (QKD) with distributed and synchronized local oscillators.⁹⁸ Studies of entanglement-based CV QKD schemes are a good starting point for estimating the distance over which quantum sensing networks would be useful because they rely on similar types of entanglement. While these network analyses usually characterize their network quality in terms of an overall data rate as limited by distance, the rate limit arises due to propagation losses and excess noise. Typical distances over

which a CV quantum network may operate while still maintaining some useful quantum correlations are of order 30–40 km, but this may be improved with the use of preamplification before detection.⁹⁹ On the other hand, quantum repeaters, which are not yet available in practice, may be used to extend this distance by more than an order of magnitude.¹⁰⁰

PERSPECTIVE AND OUTLOOK

In this Perspective, we provided examples of quantum sensing with single-mode and two-mode squeezed states. In recent years, these examples have moved beyond proofs-of-principle to the point of detecting classically inaccessible signals in laboratory settings. Moving forward, the most immediate task in quantum sensing with squeezed light is to improve the quantum noise reduction further. Many quantum optics sources are limited to 10 dB of quantum noise reduction below the SNL, and losses inherent in the sensors limit the amount of observable squeezing to only a few decibels at present. Reducing the loss is possible, as the past decade of sensing has demonstrated, and improving the squeezing to very large levels has also been demonstrated.²⁸ With continued improvements it is likely that an order of magnitude in noise reduction for a practical optical sensor will be attained in the near future, which will directly improve SNR. To extend gains in SNR further, novel detection techniques that make use of squeezing, quantum anticorrelations, and cross-correlation measurements will be required. In addition, chip-scale integration of squeezed light sources will be critical to optimizing the cost, size, weight, and power of these quantum sensors.

Further ahead, the Heisenberg limit will be possible with distributed squeezing across many optical nodes. Quantum networks offer the potential for transformative advances. As the breadth of applications presented in this perspective demonstrate, future quantum sensors are likely to impact a wide variety of fields, including new approaches to gravitational wave sensing.^{20,101} For instance, networks of squeezed states may be used to enable quantum enhanced timing resolution in geographically remote optical atomic clocks, resulting in a single international clock with quantum-enabled stability, accuracy, and security. These techniques may even enable the development of an entangled network of microwave detectors for cosmology applications and dark matter detection.¹⁰²

Quantum sensing with squeezed light, therefore, has come a long way from the original 1981 interferometry proposal. It has established its usefulness for multiple applications including imaging, plasmonics, magnetometry, and beam displacement measurements. After years of facing the limitations of losses and low squeezing, the field has entered into a renaissance, which will only be accelerated by the dawn of widespread entanglement and quantum networks.

AUTHOR INFORMATION

Corresponding Authors

*E-mail: lawriejb@ornl.gov.

*E-mail: paul.lett@nist.gov.

*E-mail: marino@ou.edu.

*E-mail: pooserrc@ornl.gov.

ORCID

B. J. Lawrie: 0000-0003-1431-066X

Notes

This manuscript has been authored by UT-Battelle, LLC, under Contract No. DE-AC05-00OR22725 with the U.S. Department of Energy. The United States Government retains and the publisher, by accepting the article for publication, acknowledges that the United States Government retains a non-exclusive, paid-up, irrevocable, worldwide license to publish or reproduce the published form of this manuscript, or allow others to do so, for United States Government purposes. The Department of Energy will provide public access to these results of federally sponsored research in accordance with the DOE Public Access Plan (<http://energy.gov/downloads/doe-public-access-plan>).

The authors declare no competing financial interest.

ACKNOWLEDGMENTS

The authors acknowledge support from the W.M. Keck Foundation and from the Laboratory Directed Research and Development program. This work was performed in part at Oak Ridge National Laboratory, operated by UT-Battelle for the U.S. Department of Energy under contract no. DE-AC05-00OR22725. P.D.L. acknowledges support from National Science Foundation (NSF) Grant 1708036 and Air Force Office of Scientific Research (AFOSR) Grant FA9550-16-1-0423.

REFERENCES

- (1) Slusher, R. E.; Hollberg, L. W.; Yurke, B.; Mertz, J. C.; Valley, J. F. Observation of Squeezed States Generated by Four-Wave Mixing in an Optical Cavity. *Phys. Rev. Lett.* **1985**, *55*, 2409–2412.
- (2) Wu, L.-A.; Kimble, H.; Hall, J.; Wu, H. Generation of squeezed states by parametric down conversion. *Phys. Rev. Lett.* **1986**, *57*, 2520.
- (3) Shelby, R.; Levenson, M.; Perlmutter, S.; DeVoe, R.; Walls, D. Broad-band parametric deamplification of quantum noise in an optical fiber. *Phys. Rev. Lett.* **1986**, *57*, 691.
- (4) Machida, S.; Yamamoto, Y.; Itaya, Y. Observation of amplitude squeezing in a constant-current-driven semiconductor laser. *Phys. Rev. Lett.* **1987**, *58*, 1000.
- (5) Caves, C. M. Quantum-mechanical noise in an interferometer. *Phys. Rev. D: Part. Fields* **1981**, *23*, 1693–1708.
- (6) Grangier, P.; Slusher, R.; Yurke, B.; LaPorta, A. Squeezed-light-enhanced polarization interferometer. *Phys. Rev. Lett.* **1987**, *59*, 2153.
- (7) Polzik, E.; Carri, J.; Kimble, H. Spectroscopy with squeezed light. *Phys. Rev. Lett.* **1992**, *68*, 3020.
- (8) Polzik, E.; Carri, J.; Kimble, H. Atomic spectroscopy with squeezed light for sensitivity beyond the vacuum-state limit. *Appl. Phys. B: Photophys. Laser Chem.* **1992**, *55*, 279–290.
- (9) Pooser, R. C.; Lawrie, B. Ultrasensitive measurement of microcantilever displacement below the shot-noise limit. *Optica* **2015**, *2*, 393–399.
- (10) Dowran, M.; Kumar, A.; Lawrie, B. J.; Pooser, R. C.; Marino, A. M. Quantum-enhanced plasmonic sensing. *Optica* **2018**, *5*, 628–633.
- (11) Aasi, J.; et al. Enhancing the sensitivity of the LIGO gravitational wave detector by using squeezed states of light. *Nat. Photonics* **2013**, *7*, 613–619.
- (12) Lawrie, B. J.; Evans, P. G.; Pooser, R. C. Extraordinary optical transmission of multimode quantum correlations via localized surface plasmons. *Phys. Rev. Lett.* **2013**, *110*, 156802.
- (13) Huck, A.; Smolka, S.; Lodahl, P.; Sørensen, A. S.; Boltasseva, A.; Janousek, J.; Andersen, U. L. Demonstration of Quadrature-Squeezed Surface Plasmons in a Gold Waveguide. *Phys. Rev. Lett.* **2009**, *102*, 246802.
- (14) Fan, W.; Lawrie, B. J.; Pooser, R. C. Quantum plasmonic sensing. *Phys. Rev. A: At., Mol., Opt. Phys.* **2015**, *92*, No. 053812.
- (15) Hoff, U. B.; Harris, G. I.; Madsen, L. S.; Kerdoncuff, H.; Lassen, M.; Nielsen, B. M.; Bowen, W. P.; Andersen, U. L. Quantum-

enhanced micromechanical displacement sensitivity. *Opt. Lett.* **2013**, *38*, 1413–1415.

(16) Lloyd, S. Enhanced sensitivity of photodetection via quantum illumination. *Science* **2008**, *321*, 1463–1465.

(17) Tan, S.-H.; Erkmen, B. I.; Giovannetti, V.; Guha, S.; Lloyd, S.; Maccone, L.; Pirandola, S.; Shapiro, J. H. Quantum illumination with Gaussian states. *Phys. Rev. Lett.* **2008**, *101*, 253601.

(18) Zhang, Z.; Mouradian, S.; Wong, F. N.; Shapiro, J. H. Entanglement-enhanced sensing in a lossy and noisy environment. *Phys. Rev. Lett.* **2015**, *114*, 110506.

(19) Zhuang, Q.; Zhang, Z.; Shapiro, J. H. Optimum mixed-state discrimination for noisy entanglement-enhanced sensing. *Phys. Rev. Lett.* **2017**, *118*, No. 040801.

(20) Komar, P.; Kessler, E. M.; Bishof, M.; Jiang, L.; Sørensen, A. S.; Ye, J.; Lukin, M. D. A quantum network of clocks. *Nat. Phys.* **2014**, *10*, 582.

(21) Leibfried, D.; Barrett, M. D.; Schaetz, T.; Britton, J.; Chiaverini, J.; Itano, W. M.; Jost, J. D.; Langer, C.; Wineland, D. J. Toward Heisenberg-limited spectroscopy with multiparticle entangled states. *Science* **2004**, *304*, 1476–1478.

(22) Taylor, M. A.; Janousek, J.; Daria, V.; Knittel, J.; Hage, B.; Bachor, H.-A.; Bowen, W. P. Biological measurement beyond the quantum limit. *Nat. Photonics* **2013**, *7*, 229–233.

(23) Taylor, M. A.; Janousek, J.; Daria, V.; Knittel, J.; Hage, B.; Bachor, H.-A.; Bowen, W. P. Subdiffraction-limited quantum imaging within a living cell. *Phys. Rev. X* **2014**, *4*, No. 011017.

(24) Treps, N.; Grosse, N.; Bowen, W. P.; Fabre, C.; Bachor, H.-A.; Lam, P. K. A quantum laser pointer. *Science* **2003**, *301*, 940–943.

(25) Treps, N.; Delaubert, V.; Maitre, A.; Courty, J. M.; Fabre, C. Quantum noise in multipixel image processing. *Phys. Rev. A: At., Mol., Opt. Phys.* **2005**, *71*, No. 013820.

(26) Treps, N.; Andersen, U.; Buchler, B.; Lam, P. K.; Maitre, A.; Bachor, H.-A.; Fabre, C. Surpassing the standard quantum limit for optical imaging using nonclassical multimode light. *Phys. Rev. Lett.* **2002**, *88*, 203601.

(27) Schnabel, R.; Mavalvala, N.; McClelland, D. E.; Lam, P. K. Quantum metrology for gravitational wave astronomy. *Nat. Commun.* **2010**, *1*, 121.

(28) Vahlbruch, H.; Mehmet, M.; Danzmann, K.; Schnabel, R. Detection of 15 dB squeezed states of light and their application for the absolute calibration of photoelectric quantum efficiency. *Phys. Rev. Lett.* **2016**, *117*, 110801.

(29) Goda, K.; Miyakawa, O.; Mikhailov, E.; Saraf, S.; Adhikari, R.; McKenzie, K.; Ward, R.; Vass, S.; Weinstein, A.; Mavalvala, N. A quantum-enhanced prototype gravitational-wave detector. *Nat. Phys.* **2008**, *4*, 472–476.

(30) Brida, G.; Genovese, M.; Ruo Berchera, I. Experimental realization of sub-shot-noise quantum imaging. *Nat. Photonics* **2010**, *4*, 227–230.

(31) Lee, J.-S.; Huynh, T.; Lee, S.-Y.; Lee, K.-G.; Lee, J.; Tame, M.; Rockstuhl, C.; Lee, C. Quantum noise reduction in intensity-sensitive surface-plasmon-resonance sensors. *Phys. Rev. A: At., Mol., Opt. Phys.* **2017**, *96*, No. 033833.

(32) Lawrie, B.; Pooser, R. C. Toward real-time quantum imaging with a single pixel camera. *Opt. Express* **2013**, *21*, 7549–7559.

(33) Pooser, R. C.; Lawrie, B. Plasmonic trace sensing below the photon shot noise limit. *ACS Photonics* **2016**, *3*, 8–13.

(34) Pinel, O.; Fade, J.; Braun, D.; Jian, P.; Treps, N.; Fabre, C. Ultimate sensitivity of precision measurements with intense Gaussian quantum light: A multimodal approach. *Phys. Rev. A: At., Mol., Opt. Phys.* **2012**, *85*, No. 010101.

(35) Armstrong, S.; Morizur, J.-F.; Janousek, J.; Hage, B.; Treps, N.; Lam, P. K.; Bachor, H.-A. Programmable multimode quantum networks. *Nat. Commun.* **2012**, *3*, 1026.

(36) Christ, A.; Lupo, C.; Silberhorn, C. Exponentially enhanced quantum communication rate by multiplexing continuous-variable teleportation. *New J. Phys.* **2012**, *14*, No. 083007.

(37) Holtfrerich, M. W.; Dowran, M.; Davidson, R.; Lawrie, B. J.; Pooser, R. C.; Marino, A. M. Toward quantum plasmonic networks. *Optica* **2016**, *3*, 985–988.

(38) Boyer, V.; Marino, A. M.; Pooser, R. C.; Lett, P. D. Entangled images from four-wave mixing. *Science* **2008**, *321*, 544–547.

(39) Lawrie, B. J.; Yang, Y.; Eaton, M.; Black, A. N.; Pooser, R. C. Robust and compact entanglement generation from diode-laser-pumped four-wave mixing. *Appl. Phys. Lett.* **2016**, *108*, 151107.

(40) Marino, A. M.; Pooser, R. C.; Boyer, V.; Lett, P. D. Tunable delay of Einstein–Podolsky–Rosen entanglement. *Nature* **2009**, *457*, 859–862.

(41) Menicucci, N. C.; Flammia, S. T.; Zaidi, H.; Pfister, O. Ultracompact generation of continuous-variable cluster states. *Phys. Rev. A: At., Mol., Opt. Phys.* **2007**, *76*, No. 010302.

(42) Pfister, O.; Feng, S.; Jennings, G.; Pooser, R.; Xie, D. Multipartite continuous-variable entanglement from concurrent nonlinearities. *Phys. Rev. A: At., Mol., Opt. Phys.* **2004**, *70*, No. 020302.

(43) Yokoyama, S.; Ukai, R.; Armstrong, S. C.; Sornphiphatphong, C.; Kaji, T.; Suzuki, S.; Yoshikawa, J.-i.; Yonezawa, H.; Menicucci, N. C.; Furusawa, A. Ultra-large-scale continuous-variable cluster states multiplexed in the time domain. *Nat. Photonics* **2013**, *7*, 982.

(44) Yoshikawa, J.-i.; Yokoyama, S.; Kaji, T.; Sornphiphatphong, C.; Shiozawa, Y.; Makino, K.; Furusawa, A. Invited Article: Generation of one-million-mode continuous-variable cluster state by unlimited time-domain multiplexing. *APL Photonics* **2016**, *1*, No. 060801.

(45) Ukai, R.; Iwata, N.; Shimokawa, Y.; Armstrong, S. C.; Politi, A.; Yoshikawa, J.-i.; van Loock, P. v.; Furusawa, A. Demonstration of unconditional one-way quantum computations for continuous variables. *Phys. Rev. Lett.* **2011**, *106*, 240504.

(46) Gu, M.; Weedbrook, C.; Menicucci, N. C.; Ralph, T. C.; van Loock, P. Quantum computing with continuous-variable clusters. *Phys. Rev. A: At., Mol., Opt. Phys.* **2009**, *79*, No. 062318.

(47) Chen, M.; Menicucci, N. C.; Pfister, O. Experimental realization of multipartite entanglement of 60 modes of a quantum optical frequency comb. *Phys. Rev. Lett.* **2014**, *112*, 120505.

(48) Pezzé, L.; Smerzi, A. Mach-Zehnder interferometry at the Heisenberg limit with coherent and squeezed-vacuum light. *Phys. Rev. Lett.* **2008**, *100*, No. 073601.

(49) Bondurant, R. S.; Shapiro, J. H. Squeezed states in phase-sensing interferometers. *Phys. Rev. D: Part. Fields* **1984**, *30*, 2548.

(50) Grote, H.; Danzmann, K.; Dooley, K. L.; Schnabel, R.; Slutsky, J.; Vahlbruch, H. First Long-Term Application of Squeezed States of Light in a Gravitational-Wave Observatory. *Phys. Rev. Lett.* **2013**, *110*, 181101.

(51) Lucivero, V. G.; Jiménez-Martínez, R.; Kong, J.; Mitchell, M. W. Squeezed-light spin noise spectroscopy. *Phys. Rev. A: At., Mol., Opt. Phys.* **2016**, *93*, No. 053802.

(52) Li, B.-B.; Bilek, J.; Hoff, U. B.; Madsen, L. S.; Forstner, S.; Prakash, V.; Schäfermeier, C.; Gehring, T.; Bowen, W. P.; Andersen, U. L. Quantum enhanced optomechanical magnetometry. *Optica* **2018**, *5*, 850–856.

(53) Szigeti, S. S.; Tonekaboni, B.; Lau, W. Y. S.; Hood, S. N.; Haine, S. A. Squeezed-light-enhanced atom interferometry below the standard quantum limit. *Phys. Rev. A: At., Mol., Opt. Phys.* **2014**, *90*, No. 063630.

(54) Sheng, D.; Li, S.; Dural, N.; Romalis, M. V. Subfemtotesla Scalar Atomic Magnetometry Using Multipass Cells. *Phys. Rev. Lett.* **2013**, *110*, 160802.

(55) Wolfgramm, F.; Cere, A.; Beduini, F. A.; Predojević, A.; Koschorreck, M.; Mitchell, M. W. Squeezed-light optical magnetometry. *Phys. Rev. Lett.* **2010**, *105*, No. 053601.

(56) Horrom, T.; Singh, R.; Dowling, J. P.; Mikhailov, E. E. Quantum-enhanced magnetometer with low-frequency squeezing. *Phys. Rev. A: At., Mol., Opt. Phys.* **2012**, *86*, No. 023803.

(57) Bowen, W. P.; Schnabel, R.; Bachor, H.-A.; Lam, P. K. Polarization squeezing of continuous variable Stokes parameters. *Phys. Rev. Lett.* **2002**, *88*, No. 093601.

(58) Zapasskii, V. S. Spin-noise spectroscopy: from proof of principle to applications. *Adv. Opt. Photonics* **2013**, *5*, 131–168.

- (59) Motazedifard, A.; Bemani, F.; Naderi, M.; Roknizadeh, R.; Vitali, D. Force sensing based on coherent quantum noise cancellation in a hybrid optomechanical cavity with squeezed-vacuum injection. *New J. Phys.* **2016**, *18*, No. 073040.
- (60) Iwasawa, K.; Makino, K.; Yonezawa, H.; Tsang, M.; Davidovic, A.; Huntington, E.; Furusawa, A. Quantum-limited mirror-motion estimation. *Phys. Rev. Lett.* **2013**, *111*, 163602.
- (61) Otterstrom, N.; Pooser, R. C.; Lawrie, B. J. Nonlinear optical magnetometry with accessible in situ optical squeezing. *Opt. Lett.* **2014**, *39*, 6533–6536.
- (62) Kawata, S.; Inouye, Y.; Verma, P. Plasmonics for near-field nano-imaging and superlensing. *Nat. Photonics* **2009**, *3*, 388–394.
- (63) Ozbay, E. Plasmonics: Merging Photonics and Electronics at Nanoscale Dimensions. *Science* **2006**, *311*, 189–193.
- (64) Altwischer, E.; van Exter, M.; Woerdman, J. Plasmon-assisted transmission of entangled photons. *Nature* **2002**, *418*, 304–306.
- (65) Yang, T.; Ho, H. P. Computational investigation of nanohole array based SPR sensing using phase shift. *Opt. Express* **2009**, *17*, 11205–11216.
- (66) Zayats, A. V.; Smolyaninov, I. I. Near-field photonics: surface plasmon polaritons and localized surface plasmons. *J. Opt. A: Pure Appl. Opt.* **2003**, *5*, S16.
- (67) Lawrie, B. J.; Evans, P. G.; Pooser, R. C. Local surface plasmon mediated extraordinary optical transmission of multi-spatial-mode quantum noise reduction. *Phys. Rev. Lett.* **2013**, *110*, 156802.
- (68) Wang, X.; Jefferson, M.; Hobbs, P. C.; Risk, W. P.; Feller, B. E.; Miller, R. D.; Knoesen, A. Shot-noise limited detection for surface plasmon sensing. *Opt. Express* **2011**, *19*, 107–117.
- (69) Kretschmann, E.; Raether, H. Radiative decay of non radiative surface plasmons excited by light. *Z. Naturforsch., A: Phys. Sci.* **1968**, *23*, 2135–2136.
- (70) Kaya, S.; Weeber, J.-C.; Zacharatos, F.; Hassan, K.; Bernardin, T.; Cluzel, B.; Fatome, J.; Finot, C. Photo-thermal modulation of surface plasmon polariton propagation at telecommunication wavelengths. *Opt. Express* **2013**, *21*, 22269–22284.
- (71) Robinson, H. D.; Magill, B. A.; Guo, X.; Reyes, R. L.; See, E. M.; Davis, R. M.; Santos, W. L. Two-photon activation of o-nitrobenzyl ligands bound to gold surfaces. *Proc. SPIE* **2014**, 916336–916336.
- (72) Beckey, J.; Lawrie, B.; Pooser, R. C. Equivalence of differential beam displacement and truncated nonlinear interferometry. Unpublished work.
- (73) Kumar, A.; Nunley, H.; Marino, A. M. Observation of spatial quantum correlations in the macroscopic regime. *Phys. Rev. A: At., Mol., Opt. Phys.* **2017**, *95*, No. 053849.
- (74) Lawrie, B. J.; Otterstrom, N.; Pooser, R. Coherence area profiling in multi-spatial-mode squeezed states. *J. Mod. Opt.* **2016**, *63*, 989–994.
- (75) Holtfrerich, M. W.; Marino, A. M. Control of the size of the coherence area in entangled twin beams. *Phys. Rev. A: At., Mol., Opt. Phys.* **2016**, *93*, No. 063821.
- (76) Clark, J. B.; Zhou, Z.; Glorieux, Q.; Marino, A. M.; Lett, P. D. Imaging using quantum noise properties of light. *Opt. Express* **2012**, *20*, 17050–17058.
- (77) Marino, A. M.; Clark, J. B.; Glorieux, Q.; Lett, P. D. Extracting spatial information from noise measurements of multi-spatial-mode quantum states. *Eur. Phys. J. D* **2012**, *66*, 288.
- (78) Demkowicz-Dobrzański, R.; Kołodyński, J.; Guţă, M. The elusive Heisenberg limit in quantum-enhanced metrology. *Nat. Commun.* **2012**, *3*, 1063.
- (79) Chua, S.; Slagmolen, B.; Shaddock, D.; McClelland, D. Quantum squeezed light in gravitational-wave detectors. *Classical Quantum Gravity* **2014**, *31*, 183001.
- (80) Harms, J.; Chen, Y.; Chelkowski, S.; Franzen, A.; Vahlbruch, H.; Danzmann, K.; Schnabel, R. Squeezed-input, optical-spring, signal-recycled gravitational-wave detectors. *Phys. Rev. D: Part. Fields* **2003**, *68*, No. 042001.
- (81) Kimble, H. J.; Levin, Y.; Matsko, A. B.; Thorne, K. S.; Vyatchanin, S. P. Conversion of conventional gravitational-wave interferometers into quantum nondemolition interferometers by modifying their input and/or output optics. *Phys. Rev. D: Part. Fields* **2001**, *65*, No. 022002.
- (82) Ast, M.; Steinlechner, S.; Schnabel, R. Reduction of Classical Measurement Noise via Quantum-Dense Metrology. *Phys. Rev. Lett.* **2016**, *117*, 180801.
- (83) Gupta, P.; Schmittberger, B. L.; Anderson, B. E.; Jones, K. M.; Lett, P. D. Optimized phase sensing in a truncated SU(1,1) interferometer. *Opt. Express* **2018**, *26*, 391–401.
- (84) Yurke, B.; McCall, S. L.; Klauder, J. R. SU (2) and SU (1, 1) interferometers. *Phys. Rev. A: At., Mol., Opt. Phys.* **1986**, *33*, 4033.
- (85) Hudelist, F.; Kong, J.; Liu, C.; Jing, J.; Ou, Z.; Zhang, W. Quantum metrology with parametric amplifier-based photon correlation interferometers. *Nat. Commun.* **2014**, *5*, 3049.
- (86) Anderson, B. E.; Gupta, P.; Schmittberger, B. L.; Horrom, T.; Hermann-Avigliano, C.; Jones, K. M.; Lett, P. D. Phase sensing beyond the standard quantum limit with a variation on the SU(1,1) interferometer. *Optica* **2017**, *4*, 752–756.
- (87) Manceau, M.; Leuchs, G.; Khalili, F.; Chekhova, M. Detection loss tolerant supersensitive phase measurement with an SU (1, 1) interferometer. *Phys. Rev. Lett.* **2017**, *119*, 223604.
- (88) Lukens, J. M.; Pooser, R. C.; Peters, N. A. A broadband fiber-optic nonlinear interferometer. *Appl. Phys. Lett.* **2018**, *113*, No. 091103.
- (89) Mehmet, M.; Eberle, T.; Steinlechner, S.; Vahlbruch, H.; Schnabel, R. Demonstration of a quantum-enhanced fiber Sagnac interferometer. *Opt. Lett.* **2010**, *35*, 1665–1667.
- (90) Proctor, T. J.; Knott, P. A.; Dunningham, J. A. Multiparameter estimation in networked quantum sensors. *Phys. Rev. Lett.* **2018**, *120*, No. 080501.
- (91) Zhuang, Q.; Zhang, Z.; Shapiro, J. H. Distributed quantum sensing using continuous-variable multipartite entanglement. *Phys. Rev. A: At., Mol., Opt. Phys.* **2018**, *97*, No. 032329.
- (92) Pfister, O.; Feng, S.; Jennings, G.; Pooser, R.; Xie, D. Multipartite continuous-variable entanglement from concurrent nonlinearities. *Phys. Rev. A: At., Mol., Opt. Phys.* **2004**, *70*, No. 020302.
- (93) Einstein, A.; Podolsky, B.; Rosen, N. Can quantum-mechanical description of physical reality be considered complete? *Phys. Rev.* **1935**, *47*, 777.
- (94) van Loock, P.; Weedbrook, C.; Gu, M. Building Gaussian cluster states by linear optics. *Phys. Rev. A: At., Mol., Opt. Phys.* **2007**, *76*, No. 032321.
- (95) Zhang, J.; Braunstein, S. L. Continuous-variable Gaussian analog of cluster states. *Phys. Rev. A: At., Mol., Opt. Phys.* **2006**, *73*, No. 032318.
- (96) Eldredge, Z.; Foss-Feig, M.; Gross, J. A.; Rolston, S. L.; Gorshkov, A. V. Optimal and secure measurement protocols for quantum sensor networks. *Phys. Rev. A: At., Mol., Opt. Phys.* **2018**, *97*, No. 042337.
- (97) Xia, Y.; Zhuang, Q.; Clark, W.; Zhang, Z. Repeater-enhanced distributed quantum sensing based on continuous-variable multipartite entanglement. *Phys. Rev. A: At., Mol., Opt. Phys.* **2019**, *99*, No. 012328.
- (98) Qi, B.; Lougovski, P.; Pooser, R.; Grice, W.; Bobrek, M. Generating the Local Oscillator Locally in Continuous-Variable Quantum Key Distribution Based on Coherent Detection. *Phys. Rev. X* **2015**, *5*, 041009.
- (99) Fossier, S.; Diamanti, E.; Debuisschert, T.; Tualle-Brouiri, R.; Grangier, P. Improvement of continuous-variable quantum key distribution systems by using optical preamplifiers. *J. Phys. B: At., Mol. Opt. Phys.* **2009**, *42*, 114014.
- (100) Furrer, F.; Munro, W. J. Repeaters for continuous-variable quantum communication. *Phys. Rev. A: At., Mol., Opt. Phys.* **2018**, *98*, No. 032335.
- (101) Polzik, E. S.; Ye, J. Entanglement and spin squeezing in a network of distant optical lattice clocks. *Phys. Rev. A: At., Mol., Opt. Phys.* **2016**, *93*, No. 021404.
- (102) Habib, M. G.-S. L. S.; Hubmayr, H.; Irwin, K.; Kusaka, A.; Lykken, J. Quantum Sensing for High Energy Physics. **2018**,

arXiv:1803.11306. arXiv.org e-Print archive. <https://arxiv.org/abs/1803.11306>.